

# EWSR1-SMAD3–rearranged Fibroblastic Tumor

## An Emerging Entity in an Increasingly More Complex Group of Fibroblastic/Myofibroblastic Neoplasms

Michael Michal, MD,\*†‡ Ryan S. Berry, MD,§ Brian P. Rubin, MD,§ Scott E. Kilpatrick, MD,§ Abbas Agaimy, MD,|| Dmitry V. Kazakov, MD,\*‡ Petr Steiner, MD,\*‡ Nikola Ptakova, MSc,\*‡ Petr Martinek, PhD,\*‡ Ladislav Hadravsky, PhD,¶ Kvetoslava Michalova, PhD,\*‡ Zoltan Szep, PhD,# and Michal Michal, MD\*‡

**Abstract:** Three cases of superficial acral fibroblastic spindle cell neoplasms with *EWSR1-SMAD3* fusion have been recently reported. Their differential diagnosis is broad, primarily comprising rare tumors from the fibroblastic/myofibroblastic category. The aim of this report is to present 4 new cases of this entity and to discuss the appropriate differential diagnosis. Also, as the ERG antibody seems to be a characteristic marker for these tumors, we analyzed ERG immunostaining characteristics in potential mimics of this entity. All cases in our cohort occurred in women aged 5 to 68 years (mean, 36.5 y). Two were located on the hand, 1 on foot, and the last case arose on the calf. The tumor size ranged from 1 to 1.5 cm in the greatest dimension, with a mean size of 1.2 cm. Except for one recent case, follow-up was available, ranging from 7 to 18 years (mean, 11.7 y), with a recurrence noted in 1 case after 10 years. All tumors were subcutaneous and showed 2 main components. One consisted of bland, spindled cells with elongated nuclei which were round when observed on the cross-section. These cells mostly grew in relatively hypercellular, well-organized, and intersecting fascicles. The second component was prominently hyalinized and paucicellular, but lacked calcifications. Both components showed either a distinct zonation pattern, or they were randomly intermingled with each other. In all 3 analyzable tumors, next-generation sequencing showed *EWSR1-SMAD3* gene fusion in

each case. By fluorescence in situ hybridization, one tested case also revealed unbalanced rearrangement of the *EWSR1* gene. All 4 cases showed strong, diffuse nuclear expression of ERG, whereas none of the mimics stained with this antibody except for weak to moderate staining in calcifying aponeurotic fibromas (9/10 cases). Two tumors showed focal weak to moderate expression of SAT-B2. The 4 herein presented cases further broaden the clinicopathologic spectrum of tumors with *EWSR1-SMAD3* gene fusion. They also confirm that they represent a novel entity for which we propose the name *EWSR1-SMAD3*–rearranged fibroblastic Tumor. Our study also proves that in the context of fibroblastic/myofibroblastic tumors, ERG immunohistochemistry is a relatively specific marker for these neoplasms.

**Key Words:** soft tissues, acral fibroblastic spindle cell neoplasm, *EWSR1-SMAD3*–rearranged fibroblastic tumor, ERG, lipofibromatosis, lipofibromatosis-like neural tumor, myofibroma, fibromatosis, calcifying aponeurotic fibroma

(*Am J Surg Pathol* 2018;42:1325–1333)

Although several new entities have been defined or redefined during the last few decades, still there are mesenchymal neoplasms which elude precise classification. This is particularly true for soft tissue neoplasms featuring undifferentiated-looking spindled or round cells. Next-generation sequencing (NGS) represents a very effective tool for further characterization and classification of such tumors. Using this technology, Kao et al<sup>1</sup> recently reported 3 cases of a novel acral fibroblastic spindle cell neoplasm with recurrent *EWSR1-SMAD3* gene fusion. Prompted by the characteristic histologic features of these tumors, we have searched our tumor registry files for further examples. Using immunohistochemistry (IHC), fluorescence in situ hybridization (FISH) and NGS as ancillary techniques, we identified 4 cases having very similar to identical features as the recently reported cases. This confirms that these tumors clearly represent a novel neoplastic entity for which we, for practical purposes, propose the name *EWSR1-SMAD3*–rearranged fibroblastic tumor (ESFT). ERG immunostaining appears to be a helpful marker distinguishing ESFT from its mimics.

From the \*Department of Pathology; †Biomedical Center, Charles University Faculty of Medicine in Pilsen; ‡Bioptical Laboratory Ltd, Pilsen; §Department of Pathology, First Faculty of Medicine, Charles University in Prague, Prague, Czech Republic; §Department of Pathology, Robert J. Tomsich Pathology and Laboratory Medicine Institute, Cleveland Clinic, Cleveland, OH; ||Institute of Pathology, Friedrich-Alexander University Erlangen-Nürnberg, Erlangen, Germany; and #Cytopathos Ltd, Bratislava, Slovakia.

Conflicts of Interest and Source of Funding: Supported in parts by the National Sustainability Program I (NPU I) Nr. LO1503 and by the grant SVV-2017 No. 260 391 provided by the Ministry of Education Youth and Sports of the Czech Republic. The authors have disclosed that they have no significant relationships with, or financial interest in, any commercial companies pertaining to this article.

Correspondence: Michael Michal, MD, Department of Pathology, Medical Faculty and Charles University Hospital Plzen, Charles University, Alej Svobody 80, Pilsen 323 00, Czech Republic (e-mail: michael.michal@medima.cz).

Copyright © 2018 Wolters Kluwer Health, Inc. All rights reserved.

However, the differential diagnosis contains many rare entities and their reactivity with ERG antibody is currently unknown. For this reason, we also investigated ERG expression in these rare tumors.

## MATERIALS AND METHODS

The 4 cases described in this study were retrieved from the consultation files of the authors. The clinical information was extracted from the medical records, and follow-up data obtained from the patients' medical records. To retrospectively identify appropriate cases, we searched the Pilsner Tumor Registry files using the following key-words and their combinations: soft tissues+unknown, fibromatosis+unusual, lipofibromatosis, and myofibroma. This search yielded >300 cases, which were morphologically reviewed. Three cases fulfilled the criteria as reported recently and hence were included for further studies. The fourth case was a recent consultation case. All 4 cases were stained with ERG antibody, and after yielding positive results, they were submitted for FISH and NGS testing. For the analysis of ERG immunostaining in potential mimics of ESFT, 3 cases of lipofibromatosis (LPF), 10 cases of calcifying aponeurotic fibroma (CAF), 1 case of infantile digital fibroma/fibromatosis, 6 cases of superficial fibromatosis, 8 myofibromas, and 5 monophasic synovial sarcomas (MSS) were included in the study. In all cases, paraffin blocks were available. For conventional microscopy, tissues were fixed in formalin, routinely processed, embedded in paraffin, cut into 4  $\mu$ m thick sections, and stained with hematoxylin and eosin (H&E).

## Immunohistochemistry

IHC analysis was performed using a Ventana BenchMark ULTRA (Ventana Medical System Inc., Tucson, AZ). The following primary antibodies were used: ERG (for ESFT: EPR3864, prediluted, Ventana Medical Systems Inc.; CAFs were stained at a different institution using the clone EP111, 1:500, Epitomic), SOX10 (Polyclonal, 1:100; Cell Marque), S100 (Polyclonal, prediluted; Ventana), EMA (E29, 1:400; Dako), CD34 (QBEnd/10, 1:200; Dako), SMA (1A4, 1:500; Dako), Desmin (D33, 1:200; Dako), OSCAR (IsoType:IgG2a, 1:100; Covance), AE1/3 (AE1/AE3&PCK26, prediluted; Ventana), Pan-TRK (A7H6R, 1:20, Cell Signaling), SAT-B2 (CL0276, 1:100; Sigma-Aldrich), HMB45 (HMB45, 1:400; Dako),  $\beta$ -catenin (Polyclonal, 1:150; Thermo Fischer Scientific), MUC4 (8G7, 1:200; Santa Cruz Biotechnology), Synaptophysin (SP11, prediluted; Ventana), Chromogranin (DAK-A3, 1:400; Dako), CD117 (polyclonal, 1:800; Dako), DOG1 (SP31, prediluted; Cell Marque). The primary antibodies were visualized employing the enzymes alkaline phosphatase or peroxidase as detecting systems (both purchased from Ventana Medical System Inc.).

## Molecular Genetic Studies

### Detection of *EWSR1* Rearrangement by FISH

The dual color, break apart probe consisting of a mixture of FISH DNA probes on the centromeric and the telomeric sides of the *EWSR1* gene breakpoints (Abbott Molecular), was used in this interphase FISH assay to

detect the presence of an *EWSR1* (22q12) rearrangement. 200 nuclei were scored, using the reference range of 0% to 11%.

### Detection of *EWSR-SMAD3* Fusion by NGS

Fusion Plex Solid Tumor kit (ArcherDX Inc., Boulder, CO) was used to construct a cDNA library for detecting fusion transcripts in 52 genes. All steps were performed according to the manufacturer's instructions (version of the protocol LA135.F), and the library was sequenced on an Illumina platform as described previously.<sup>2</sup>

## RESULTS

### Clinical Findings

The clinical features are summarized in Table 1. All 4 patients were women with age ranging from 5 to 68 years (mean, 36.5 y). All tumors presented in the subcutaneous soft tissues of the extremities and were equally distributed between upper and lower extremity. While 3 tumors were found at acral sites, one arose on the calf. The tumor sizes ranged from 1 to 1.5 cm in greatest dimension, with a mean size of 1.2 cm. Follow-up was available for 3 patients; one case is recent. The average duration of follow-up was 11.7 years (range 7 to 18 y). After 10 years, 1 patient had a recurrence; none had metastatic disease. The cases were initially diagnosed as LPF, fibromatosis, myofibroma or descriptively as "unusual benign spindle cell tumor." In the former 3 cases, the diagnosing pathologists always mentioned that the tumors do not represent a typical example of any entity as defined by the WHO classification of soft tissue tumors.

### Pathologic Findings

The overall histopathologic appearance of ESFT varied a little from case to case. Cases 1 and 3 were vaguely lobulated or plexiform (Fig. 1A), whereas the 2 others created a single tumorous nodule (Figs. 2A, 4A), as did the recurrence in case 1 (Fig. 1E). Case 4 was circumscribed, showing a thin fibrous capsule (Fig. 4A), while the remaining cases had an infiltrative growth pattern, at least focally, occasionally engulfing a small amount of the surrounding subcutaneous adipose tissue (Figs. 1A–F, 2A). The tumors showed 2 main components. One consisted of bland spindled cells with elongated, focally wavy nuclei (Figs. 1D, 2B, D, 3C), which were round when observed on cross-section (Figs. 2D, 3B) and did not show conspicuous nucleoli. A moderate amount of eosinophilic fibrillary cytoplasm surrounded the nuclei. These cells mostly grew in relatively hypercellular and well-organized fascicles of intermediate length that frequently intersected with each other at different angles. Pleomorphism, atypia or mitoses were absent (Figs. 1D, 2B, D). The second component had an identical cellular composition and architecture. However, these areas were prominently hyalinized and lacked calcifications with only a few viable spindled cells (Fig. 2C). Both components showed either a distinct zonation pattern with the spindle cell component located at the periphery and central hyalinization (Figs. 1B, C, 4A, B), or they randomly intermingled with each other (Figs. 2B, 3A). The primary tumor in case 1 was excised with positive surgical margins and

**TABLE 1.** Clinical, Immunohistochemical, and Molecular Genetic Features

Case	Sex/ Age (y)	Location	Duration	Size (cm)	FISH	NGS	IHC +	IHC -	Recurrence	Length of FU (y)	Original Diagnosis	Comment
1	F/5 and 15	Hand—palm	3 y	1.2 and 0.3	NA	<i>EWSR1-SMAD3</i>	ERG in both; focal SAT-B2 staining in the 2nd tumor, negative in the first tumor	SOX-10; S100; EMA; CD34; SMA; Actin E; Desmin; SAT-B2; OSCAR; Pan-TRK; SAT-B2	Yes in 10 y	18	Unusual lipofibromatosis	Incomplete excision in both the original tumor and the reexcision
2	F/68	Interphalangeal joint of the thumb	10 months	1.5×0.7×0.5	NA	<i>EWSR1-SMAD3</i>	ERG, focal SAT-B2 staining	SOX-10; S100; CD34; EMA; Desmin; OSCAR; HMB45	No	10	Unusual fibromatosis	Incomplete excision but no recurrence
3	F/39	Calf	NA	1×0.5×0.5	NA	NA	ERG	S100; EMA; CD34; SMA; Desmin; OSCAR; AE1/3 Synaptophysin; Chromogranin; CD117; DOG-1	No	7	Benign plexiform spindle cell tumor	Early reexcision—no additional tumor tissue
4	F/34	Left foot—dorsal metatarsal aspect	NA	1.1×0.8×0.5	Positive	<i>EWSR1-SMAD3</i>	ERG	SOX-10; S100; EMA; CD34; SMA; Desmin; Caldesmon; AE1/3; Beta Catenin; MUC4	Recent case	Recent	Unusual myofibroma	Slowly enlarging, painful, no history of trauma

F indicates female; FU, follow-up; NA, not available.

recurred 10 years after surgery. The recurrence showed similar morphology, without increased cellularity or pleomorphism (Fig. 1E, F). Despite again leaving positive surgical margins after reexcision, no recurrence was noted with an additional 8 years of follow-up. Similarly, in case 2 the surgical margins were positive. However, the tumor did not recur with 10 years of follow-up. In case 3, the tumor was successfully removed in toto after one immediate reexcision (suggested by the pathologist due to the incompleteness of the initial removal) with no signs of recurrence 7 years after diagnosis. The fourth case was completely excised with narrow margins, but the case is too recent for any meaningful follow-up evaluation.

### IHC Findings

The IHC results are summarized in Table 1. All cases showed strong nuclear staining for ERG (Figs. 2E, 3D, 4C). The recurrent tumor in case 1 and case 2 showed focal weak to moderate nuclear staining with SAT-B2 (Fig. 2F). Despite employing a broad IHC panel including OSCAR, CD34, Pan-TRK, along with muscle, neuroendocrine, and melanoma markers, no other expression of any antibody was noted. As summarized in Table 2, from the analyzed mimics, only 9/10 cases of CAF showed a weak to moderate ERG staining in most cells. None of other mimics stained with this marker.

### Molecular Genetic Findings

The molecular genetic results are summarized in Table 1. Because of suboptimal quality of archival tissue, FISH analysis was successfully carried out only in the most recent case 4, where it confirmed unbalanced rearrangement involving

*EWSR1* gene in 72% of nuclei. The material quality issues precluded the NGS analysis in case 3. However, we believe that despite missing molecular genetic proof for this case, both the typical ESFT morphology and strong nuclear ERG expression (with all other markers being negative) warrant inclusion of this case into the study. In the remaining cases, the characteristic *EWSR1-SMAD3* gene fusion, resulting from a t(15;22)(q22.33;q12.2) was confirmed by NGS.

### DISCUSSION

The group of fibroblastic/myofibroblastic tumors encompass a broad spectrum of entities that demonstrate overlapping morphologic and immunohistochemical features, frequently defying their accurate classification. Because of the recent vast expansion of NGS-based techniques, the molecular underpinnings of these tumors are gradually being discovered, and this knowledge may be utilized in difficult cases. Moreover, it also represents an invaluable tool for a potential delineation of novel entities from hitherto unclassifiable fibroblastic tumors. An example of the latter application is the 3 cases recently reported by Kao et al<sup>1</sup> who described a novel spindle cell tumor with recurrent *EWSR1-SMAD3* fusion (referred to as ESFT in this article) that, based on all available evidence, exhibits fibroblastic differentiation. Combining both the current and initial report, altogether 7 cases of ESFT have now been described. While most findings from the original series were confirmed by us, several novel features emerged in the current series, and despite the persisting need for more substantial patient

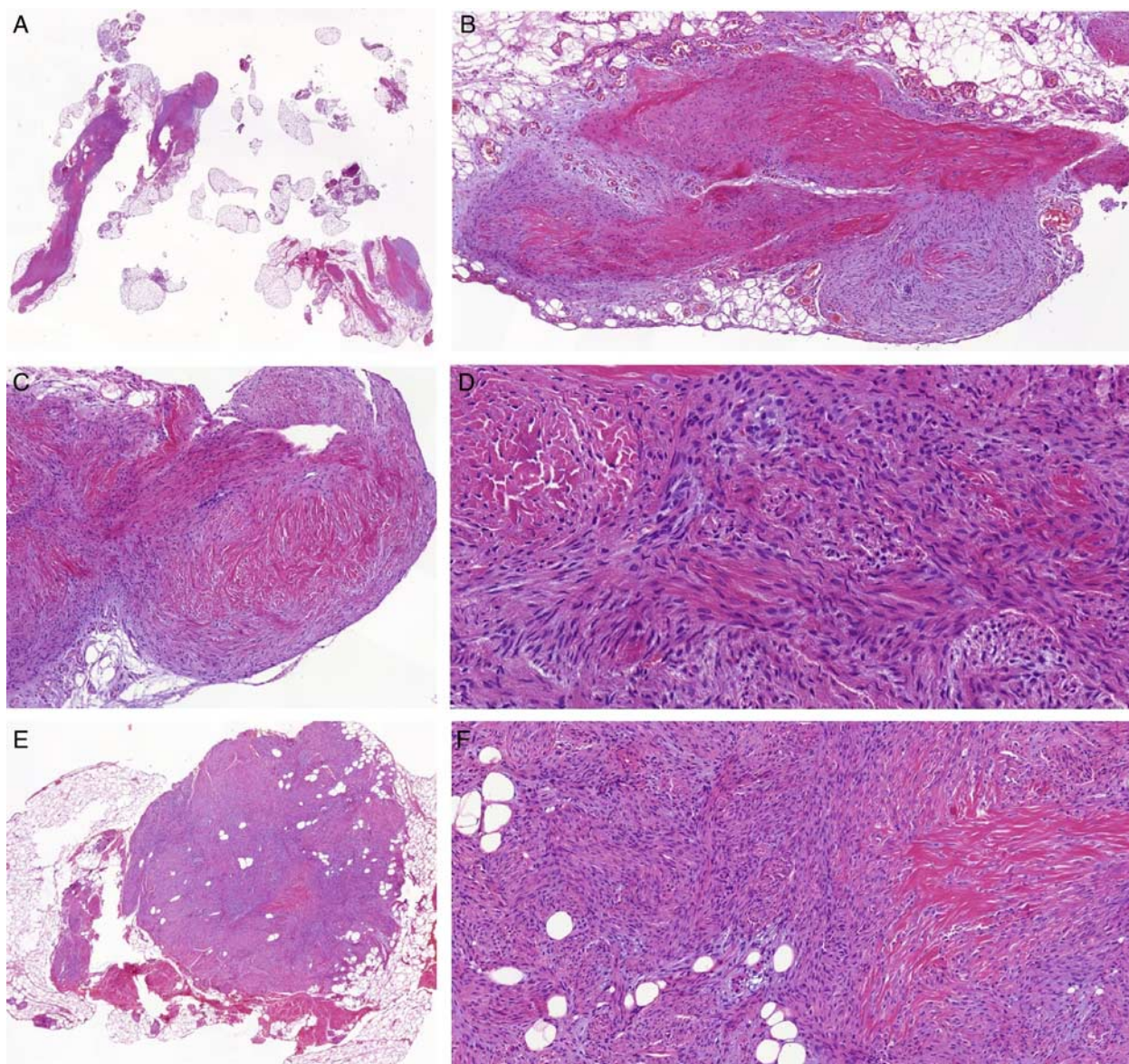


**FIGURE 1.** The original tumor in case 1 was vaguely lobulated or plexiform (A). It showed a distinct zonation pattern with central hyalinization and the spindle cell component located at the periphery, engulfing a small amount of the surrounding subcutaneous adipose tissue (B, C). Higher power view of the bland spindled cells with elongated, focally wavy nuclei growing in relatively hypercellular and well-organized fascicles of intermediate length that frequently intersected with each other at different angles (D). The recurrence created a single tumorous nodule (E), engulfing a small amount of the surrounding fat and showing the characteristic hyalinization (F).

numbers, some preliminary general observations can now be made.

The first 3 cases reported were all located at acral sites of lower extremities. Besides one of our cases that arose at the dorsal aspect of the foot, 2 other lesions were found on the acral aspects of the hand. In addition, one of the tumors in our series affected the calf, thereby representing the first nonacral case. With respect to the sex, ESFT seems to have a distinct sex predilection for women (6/7 cases). The age range is wide, with some cases arising in infants or young children, others affecting patients up to

the seventh decade. As these tumors usually grow infiltratively, they are prone to recur locally. Of the 5 cases with available follow-up, 3 (60%) have recurred after a variable time interval ranging from 5 months to as late as 10 years. In contrast, the remaining 2 cases have not recurred after long follow-up despite having positive surgical margins.

Microscopically, the low power arrangement of ESFT varied a little from the initial 3 reported cases, showing, in addition to nodular growth,<sup>1</sup> vaguely lobular or slightly plexiform tumors that infiltrated into the surrounding tissue

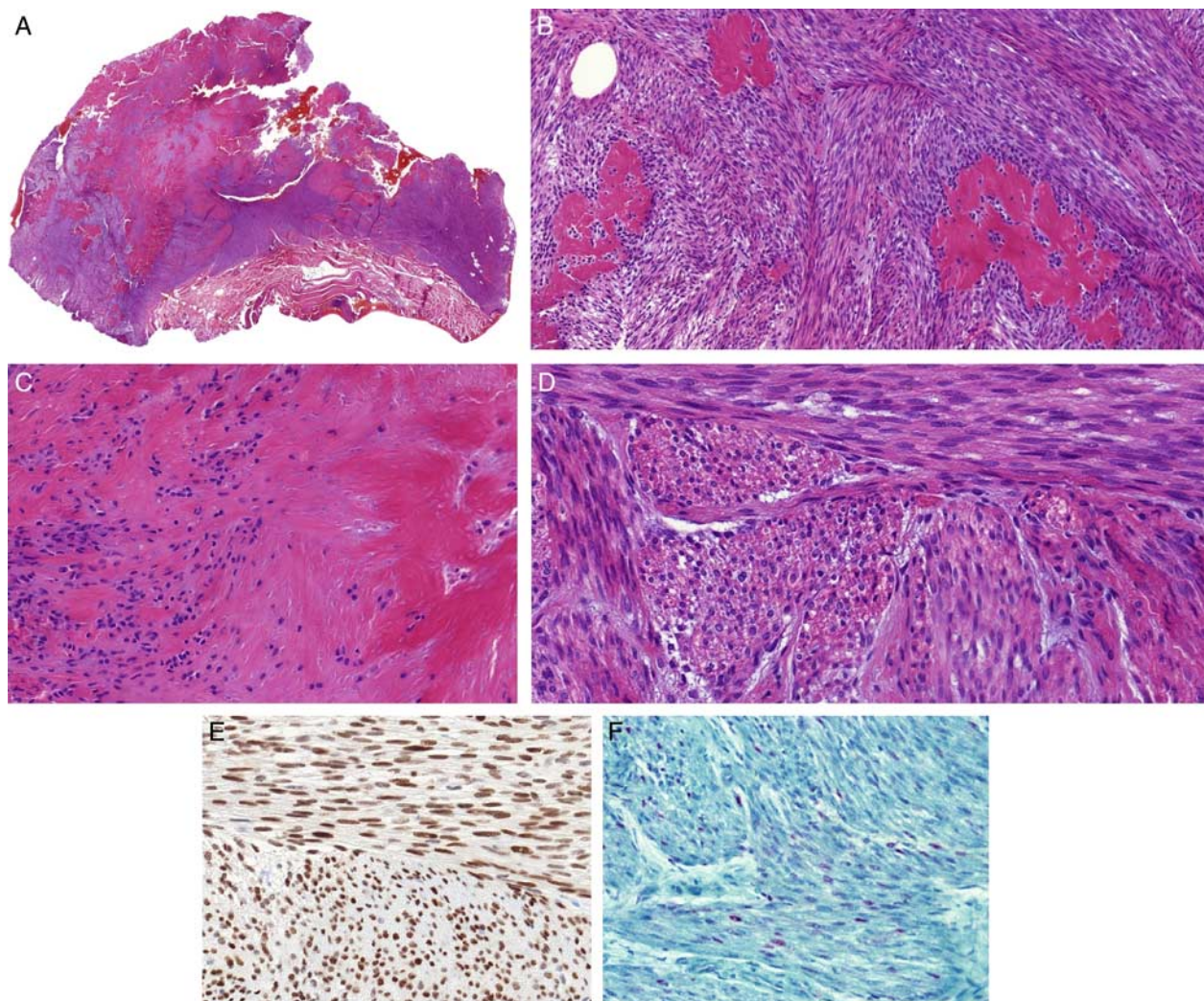


**FIGURE 2.** The tumor in case 2 created a single tumorous nodule. A small amount of engulfed adipose tissue is seen on the right (A). The hypercellular fascicles frequently intersected with each other at different angles, and in this case, randomly intermingled with the hyalinized component (B). High power view of the prominently hyalinized component that lacked calcifications with only a few viable spindled cells (C). The bland spindled cell component with elongated, focally wavy nuclei, which were round when observed on cross-section and did not show conspicuous nucleoli (D). Strong nuclear staining with ERG (E). This tumor also showed focal weak to moderate nuclear staining with SAT-B2 (F).

and showed 2 main components. The first was represented by intersecting, relatively hypercellular and well-organized fascicles of bland spindled cells. The second component had a similar cellular composition and architecture but was prominently hyalinized, and contained a small number of viable cells. In a single previously reported case, this area also featured focal stippled calcifications. The components showed either a distinct zonation pattern as reported by Kao et al,<sup>1</sup> with the spindle cell component located at the periphery and the hyalinized area in the center. In addition, in our 2 cases, the components were intermingled throughout the tumor without distinct zonation. All reported cases showed strong nuclear positivity for ERG. Although a relatively wide panel of antibodies was used in both studies, the only other reactivity observed was weak, equivocal staining with both keratins and EMA in one case of Kao et al,<sup>1</sup> and

focal weak to moderate nuclear staining with SAT-B2 in the current case 2 and in the recurrent tumor in case 1.

ERG is a widely used vascular endothelial marker and is also expressed in Ewing sarcomas or prostate carcinomas with ERG fusions.<sup>3-5</sup> Also, it was shown to be a reliable marker for chondrogenic tumors and a useful marker for phosphaturic mesenchymal tumors.<sup>6-8</sup> Its expression in fibroblastic/myofibroblastic tumors has, to our knowledge, not been described and in the right context, strong ERG expression seems to be quite specific and sensitive for ESFT. The differential diagnosis of ESFT is broad, primarily comprising rare tumors from the fibroblastic/myofibroblastic category such as LPF, CAF, lipofibromatosis-like neural tumor, myofibroma/myofibromatosis (MF), infantile digital fibroma/fibromatosis and palmar/plantar fibromatosis. In addition, MSS can also enter the differential diagnosis. Nevertheless, due to the rarity of these tumors,

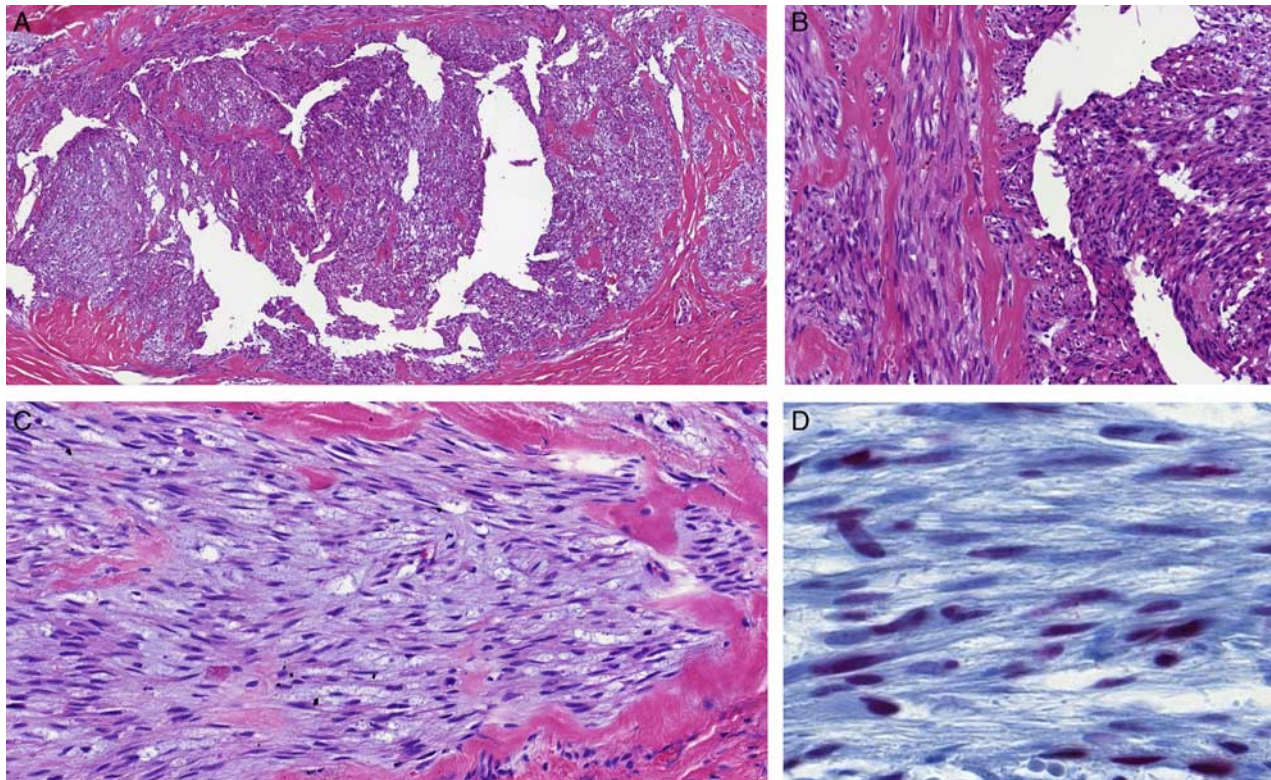


**FIGURE 3.** Both components in case 3 randomly intermingled with each other (A, B). Bland spindled cells with elongated, focally wavy nuclei (C). Strong nuclear staining with ERG (D).

their ERG expression has mostly not been studied. One of the aims of this study was thus to evaluate ERG staining in potential ESFT mimics as well.

LPF is a rare pediatric mesenchymal tumor with a predilection for the hands and feet.<sup>9</sup> ESFT frequently infiltrates the surrounding fatty tissue and may therefore be mistaken for LPF as illustrated by case 1. However, LPF does not feature the prominent hyalinized component, the fascicles do not show the prominent intersecting pattern and are composed of rather oval than fusiform cells. The fat component is also more abundant and usually present throughout the entire tumor. In contrast, the fatty component in ESFT is limited and is usually present only at the tumor margins. LPF usually stains with CD34, and about 1/3 of cases express S100 protein.<sup>9</sup> Although it may show variable staining with several other IHC markers, it does not express ERG as evidenced by our analysis carried out on 3 cases. Until recently, the molecular underpinnings of LPF were mostly unknown (discussed below).

CAF is a tumor primarily affecting children or young adults with a strong predilection for the hands and feet, although occasional examples may occur outside this typical location.<sup>10</sup> The chondroid foci of CAF bear a superficial resemblance to the hyalinized component of ESFT. However, only one case of the latter tumor was reported to contain a limited amount of calcific material. The cellularity of CAF varies, depending on the age of the lesion. However, the tumor fascicles of CAF, when present, are more

haphazardly arranged than in ESFT. Recently, *FNI-EGF* gene fusions were reported as a recurrent molecular event in the majority of CAF,<sup>11</sup> and the tumor also shows a simultaneous elevation of *FNI* mRNA levels.<sup>1</sup> ERG expression in CAF has not been reported in the literature. While confirming the specificity of strong ERG expression for ESFT among lesions in its differential diagnosis, our study also demonstrated frequent, albeit weak to moderate, expression of ERG in most (90%) of cases of CAF.

Like LPF, LPFLNT does not contain the hyalinized zones, the spindled cells are more atypical and hyperchromatic and do not show such prominent intersecting fascicles as in ESFT. Most cases stain with S100 protein and CD34, whereas ERG staining has not been reported. Recurrent *NTRK1* gene rearrangements were identified in 10/14 cases, with another 2 cases harboring *ROS1* and *ALK* gene rearrangements, respectively.<sup>12</sup> LPFLNT with *NTRK1* rearrangement is also positive with *NTRK1* IHC, which did not react in the several ESFT tested.

Interestingly, even in the absence of *FNI* fusion, one case of LPFLNT with *TPR-NTRK1* fusion showed an increased *FNI* mRNA overexpression, and even higher *FNI* mRNA upregulation was observed in ESFT. Moreover, based on unsupervised clustering of the whole transcriptome RNA data of >100 various soft tissue tumors performed by Kao et al,<sup>1</sup> CAF and ESFT clustered together with LPF and LPFLNT in one group of related tumors. *FNI* mRNA upregulation (in the presence of *FNI*

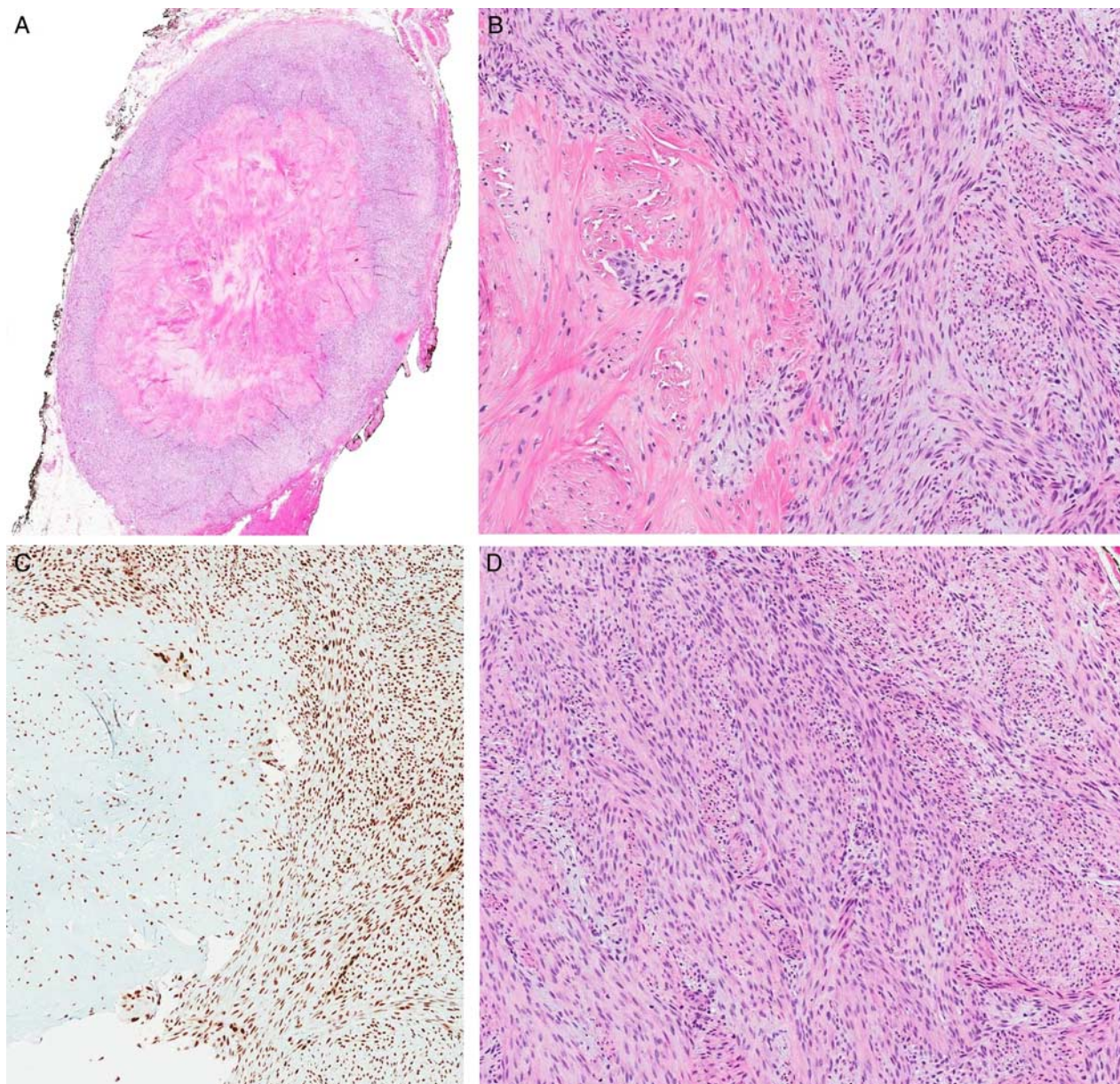


**FIGURE 4.** The tumor in case 4 created a single tumorous nodule which featured a distinct zonation pattern with the spindle cell component located at the periphery and central hyalinization (A). The prominently hyalinized component gradually merged with the more peripherally located spindle cell proliferation (B). Strong nuclear staining with ERG (C). Pleomorphism, atypia or mitoses were absent in the spindled cell component (D).

fusions) is further present in phosphaturic mesenchymal tumors which concurrently shows ERG expression.<sup>1,7,8,13,14</sup>

Very interesting findings regarding this topic were presented at the 2018 USCAP Annual Meeting in Vancouver. Prompted by a typical case of LPF that recurred showing morphologic features of CAF, Al-Ibraheemi and colleagues studied 16 cases of LPF for the CAF-associated fusion or other genetic events. They found a subset of LPF harboring the CAF-associated *FNI-EGF* fusion, or a related *FNI-TGFA* fusion, suggesting that some “LPF” may instead represent CAF lacking the hallmark calcifications. Other LPF showed alterations involving kinase-encoding genes

*TPR-ROS1* and *SPARC-PDGFRB*, suggesting a possible link to LPFLNT. A third subset of LPF showed novel gene fusions *HBEGF-RBM27* and *EGRI-GRI1*, and 6 cases lacked identifiable genetic events. Therefore, LPF appears to be a genetically heterogeneous tumor, despite stereotypical morphologic features.<sup>15</sup> Finally, it seems that ESFT, LPF, CAF, and LPFLNT represent a group of benign or locally aggressive tumors that, besides sharing overlapping morphologic features, are also related at the molecular and/or transcriptomic level. Although morphologically relatively dissimilar, phosphaturic mesenchymal tumor also seems to be vaguely related to these neoplasms.

**TABLE 2.** ERG Immunohistochemical Staining Characteristics of ESFT Mimics

Tumor (Acronym Used in the Text)	ERG Staining: Positive/ Tested Cases (Literature Data)
Lipofibromatosis (LPF)	0/3
Calcifying aponeurotic fibroma (CAF)	9/10 weak to moderate expression*
Lipofibromatosis-like neural tumor (LFLNT)	NA
Myofibroma/myofibromatosis (MF)	0/8 (ref. 3—0/9)
Infantile digital fibroma/fibromatosis	0/1
Palmar/plantar fibromatosis	0/6 (ref. 3—data for desmoid-type fibromatosis—0/19)
Monophasic synovial sarcoma (MSS)	0/5 (ref. 3—0/36)

\*Stained at different institution using the clone EP111; the rest stained with the clone EPR3864—for details see the Materials and methods section.

NA indicates not available.

MF frequently contain myointimal-like nodular proliferations (also called myoid or vascular balls).<sup>8</sup> These areas may show a variable level of hyalinization, and when well developed, they may closely mimic the hyalinized areas of ESFT. Especially in the cellular variants of MF, the surrounding spindle cells sometimes additionally acquire a hypercellular fascicular arrangement<sup>16</sup> and may thus also resemble similar areas of ESFT. Nevertheless, the spindled cells of MF are plumper, and the hemangiopericytoma-like vessels and pericytic arrangement of the surrounding cells are usually present and offer a helpful diagnostic clue. Although with variable intensity, virtually all MF express smooth muscle actin and the cellular examples also co-express desmin.<sup>17</sup> However, they do not stain with ERG as documented by our analysis of 8 cases and by the literature data.<sup>3</sup> Genetically, classic MF show *PDGFRB* mutation in most cases,<sup>8</sup> while a subset of what appears to be the cellular variant of MF was reported to show *SRF-RELA* fusion.<sup>17</sup>

Infantile digital fibroma/fibromatosis has a cellular arrangement that varies in any given tumor from whorled bundles or interlacing short fascicles to broad storiform arrays and is thus slightly different from the uniformly fascicular architecture of ESFT. Moreover, the hyalinized areas typical for ESFT are absent. The spindled tumor cells in infantile digital fibromatosis possess an elongated nucleus, lightly eosinophilic cytoplasm and mainly, the very characteristic paranuclear inclusion. They are present in most examples, and on standard HE sections appear as a small, rounded, pale pink body. The tumors uniformly stain with muscle markers,<sup>18</sup> but ERG expression was not found in our single tested case.

Although superficial fibromatosis may, particularly in the cellular examples, closely resemble ESFT, a sharp transition to juxtaposed larger hyalinized areas as seen in the latter tumor are not found. ESFT is much more cellular than examples of superficial fibromatoses, and cytologically the nuclei of ESFT are less curved, wavy, and plumper than in any type of fibromatosis. Expression of smooth muscle

actin, uniformly present in fibromatosis, is not a feature of ESFT. ERG staining has been studied in desmoid-type fibromatosis and was negative,<sup>3</sup> as was the staining of 6 cases of superficial fibromatosis in our study.

MSS commonly occurs on the extremities including the distal parts, where it may be diagnosed at a very small size.<sup>19</sup> As it often forms hypercellular fascicles of spindled cells that lack significant pleomorphism and frequently shows a variable degree of hyalinization it may mimic ESFT. However, even in MSS, areas with hints of more epithelioid growth can be found and this can usually be confirmed by IHC. The hemangiopericytomatous vasculature, prominent mast cell infiltrate and a high mitotic and proliferative index are all features strongly favoring MSS. The significant IHC differences such as EMA or keratin staining in MSS can be of great help in the distinction. Conversely, ERG is reported to be negative in MSS<sup>3</sup> and accordingly, the expression was not found in our study. FISH analysis will be rarely needed for the distinction of these 2 neoplasms.

It is known that *EWSR1* is a highly promiscuous gene that is rearranged in many different tumor types. In the context of dermal-based spindle cell neoplasms with *EWSR1* rearrangement, the diagnosis of cutaneous forms of myoepithelioma<sup>20,21</sup> or clear cell sarcoma<sup>22</sup> may also be considered. However, their overall morphology and immunoprofile differ significantly from ESFT. Lastly, a small number of spindle cell sarcomas with prominent myopericytic/hemangiopericytic growth pattern have been reported to harbor *LMNA-NTRK1* and *TPM3-NTRK1* gene fusions.<sup>23</sup> Identical fusions are present in LPLNT, and the latter fusion has also been described in one case of pediatric spindle cell sarcoma resembling infantile fibrosarcoma.<sup>24</sup> This underscores the complexity and overlapping features within the group of fibroblastic/myofibroblastic tumors. Also, it once again proves that not only tumors with the same fusion partner but even with an identical gene fusion may be morphologically and biologically completely different and that the clinical and histologic context remains crucial for establishing the correct diagnosis.

In this article, we presented 4 cases of a recently described fibroblastic mesenchymal tumor with *EWSR1-SMAD3* gene fusion, further extending its clinicopathologic spectrum. All reported examples demonstrate highly reproducible morphologic features that allow classification of this tumor on H&E slides with a high level of certainty, confirming that they represent a novel and distinct entity within the otherwise highly complex group of fibroblastic/myofibroblastic tumors. We also proved that in the right clinicopathologic context, strong ERG staining is a sensitive and relatively specific immunohistochemical marker for these tumors. For practical purposes, we propose the name *EWSR1-SMAD3*-rearranged Fibroblastic Tumor for these neoplasms.

## REFERENCES

- Kao YC, Flucke U, Eijkelenboom A, et al. Novel *EWSR1-SMAD3* gene fusions in a group of acral fibroblastic spindle cell neoplasms. *Am J Surg Pathol*. 2018;42:522–528.
- Skalova A, Vanecek T, Martinek P, et al. Molecular profiling of mammary analog secretory carcinoma revealed a subset of tumors



- harboring a novel ETV6-RET translocation: report of 10 cases. *Am J Surg Pathol*. 2018;42:234–246.
3. Miettinen M, Wang ZF, Paetau A, et al. ERG transcription factor as an immunohistochemical marker for vascular endothelial tumors and prostatic carcinoma. *Am J Surg Pathol*. 2011;35:432–441.
  4. Wang WL, Patel NR, Caragea M, et al. Expression of ERG, an Ets family transcription factor, identifies ERG-rearranged Ewing sarcoma. *Mod Pathol*. 2012;25:1378–1383.
  5. Furusato B, Tan SH, Young D, et al. ERG oncoprotein expression in prostate cancer: clonal progression of ERG-positive tumor cells and potential for ERG-based stratification. *Prostate Cancer Prostatic Dis*. 2010;13:228–237.
  6. Shon W, Folpe AL, Fritchie KJ. ERG expression in chondrogenic bone and soft tissue tumours. *J Clin Pathol*. 2015;68:125–129.
  7. Tajima S, Takashi Y, Ito N, et al. ERG and FLII are useful immunohistochemical markers in phosphaturic mesenchymal tumors. *Med Mol Morphol*. 2016;49:203–209.
  8. Agaimy A, Bieg M, Michal M, et al. Recurrent somatic PDGFRB mutations in sporadic infantile/solitary adult myofibromas but not in angioleiomyomas and myopericytomas. *Am J Surg Pathol*. 2017;41:195–203.
  9. Fetsch JF, Miettinen M, Laskin WB, et al. A clinicopathologic study of 45 pediatric soft tissue tumors with an admixture of adipose tissue and fibroblastic elements, and a proposal for classification as lipofibromatosis. *Am J Surg Pathol*. 2000;24:1491–1500.
  10. Fetsch JF, Miettinen M. Calcifying aponeurotic fibroma: a clinicopathologic study of 22 cases arising in uncommon sites. *Hum Pathol*. 1998;29:1504–1510.
  11. Puls F, Hofvander J, Magnusson L, et al. FN1-EGF gene fusions are recurrent in calcifying aponeurotic fibroma. *J Pathol*. 2016;238:502–507.
  12. Agaram NP, Zhang L, Sung YS, et al. Recurrent NTRK1 gene fusions define a novel subset of locally aggressive lipofibromatosis-like neural tumors. *Am J Surg Pathol*. 2016;40:1407–1416.
  13. Lee JC, Jeng YM, Su SY, et al. Identification of a novel FN1-FGFR1 genetic fusion as a frequent event in phosphaturic mesenchymal tumour. *J Pathol*. 2015;235:539–545.
  14. Lee JC, Su SY, Changou CA, et al. Characterization of FN1-FGFR1 and novel FN1-FGF1 fusion genes in a large series of phosphaturic mesenchymal tumors. *Mod Pathol*. 2016;29:1335–1346.
  15. Al-Ibraheemi A, Perez-Atayde A, Perry KD, et al. Lipofibromatosis (LPF): a clinicopathological and molecular genetic study of 16 cases suggesting a link to calcifying aponeurotic fibroma (CAF) and LPF-like neural tumor (LPFLNT). *Mod Pathol*. 2018;31:18.
  16. Linos K, Carter JM, Gardner JM, et al. Myofibromas with atypical features: expanding the morphologic spectrum of a benign entity. *Am J Surg Pathol*. 2014;38:1649–1654.
  17. Antonescu CR, Sung YS, Zhang L, et al. Recurrent SRF-RELA fusions define a novel subset of cellular myofibroma/myopericytoma: a potential diagnostic pitfall with sarcomas with myogenic differentiation. *Am J Surg Pathol*. 2017;41:677–684.
  18. Laskin WB, Miettinen M, Fetsch JF. Infantile digital fibroma/fibromatosis: a clinicopathologic and immunohistochemical study of 69 tumors from 57 patients with long-term follow-up. *Am J Surg Pathol*. 2009;33:1–13.
  19. Michal M, Fanburg-Smith JC, Lasota J, et al. Minute synovial sarcomas of the hands and feet: a clinicopathologic study of 21 tumors less than 1 cm. *Am J Surg Pathol*. 2006;30:721–726.
  20. Jo VY, Antonescu CR, Zhang L, et al. Cutaneous syncytial myoepithelioma: clinicopathologic characterization in a series of 38 cases. *Am J Surg Pathol*. 2013;37:710–718.
  21. Flucke U, Palmedo G, Blankenhorn N, et al. EWSR1 gene rearrangement occurs in a subset of cutaneous myoepithelial tumors: a study of 18 cases. *Mod Pathol*. 2011;24:1444–1450.
  22. Hantschke M, Mentzel T, Rutten A, et al. Cutaneous clear cell sarcoma: a clinicopathologic, immunohistochemical, and molecular analysis of 12 cases emphasizing its distinction from dermal melanoma. *Am J Surg Pathol*. 2010;34:216–222.
  23. Haller F, Knopf J, Ackermann A, et al. Paediatric and adult soft tissue sarcomas with NTRK1 gene fusions: a subset of spindle cell sarcomas unified by a prominent myopericytic/haemangiopericytic pattern. *J Pathol*. 2016;238:700–710.
  24. Kao YC, Fletcher CDM, Alaggio R, et al. Recurrent BRAF gene fusions in a subset of pediatric spindle cell sarcomas: expanding the genetic spectrum of tumors with overlapping features with infantile fibrosarcoma. *Am J Surg Pathol*. 2018;42:28–38.